RESEARCH PAPER

Preparation of $TiO_2/Cu_{0.4}Fe_{1.6}Ni_{0.65}Zn_{0.35}O_4$ Nanocomposite for Degradation of Acid Red 88 under Visible Light Irradiation

Hayfaa Raheem Abdulkareem [1], Mohanad Kadhem Alshujery [2], Mohamed Ahmed [3], Waleed Shallal [4], Aseel Niema Hafith [4]*

[1] Basra University for Oil and Gas, Chemical Engineering and Oil Refinery Department, Iraq

[2] Ministry of Education, General Directorate of Education, AL-Karkh the Second, Iraq

[3] Department of Physics, College of Science, University of Sumer, Iraq

[4] College of Dentistry, University of Kut, Wasit, 52001, Iraq

ARTICLE INFO

Article History:
Received 12 December 2025
Accepted 27 March 2026
Published 01 April 2026

Keywords:
Acid red 88
Nanocomposite
Photocatalyst
$TiO_2/Cu_{0.4}Fe_{1.6}Ni_{0.65}Zn_{0.35}O_4$
Visible light

ABSTRACT

An excellent nanocomposite comprising TiO_2 and $Cu_{0.4}Fe_{1.6}Ni_{0.65}Zn_{0.35}O_4$ (CFNZO) nanoparticles was prepared and demonstrated to be an efficient visible light photocatalyst. To verify photocatalytic potential of the prepared nanocomposite, optical characterizations were carried out using diffuse reflectance (DRS) and photoluminescence (PL) spectroscopy. The nanocomposite containing 2 wt% of CFNZO nanoparticles (TiO_2/2-CFNZO) showed a band gap value of 2.76 eV. Acid red 88 (AR88) solution was degraded using the prepared nanocomposite under the visible light irradiation for 120 min. The photocatalytic activity of the nanocomposite was carefully examined under various conditions, such as varying content of CFNZO nanoparticles, different concentrations of photocatalyst, AR88 solution pH, and H_2O_2 concentrations. Accordingly, the highest photocatalytic degradation level was achieved in acidic AR88 solution (pH = 3), using 0.04 g of TiO_2/2-CFNZO nanocomposite and 2 mL of 0.02 M H_2O_2 oxidant. Additionally, the degradation reactions performed using various radical scavenger agents confirmed that the reaction proceeded via hydroxyl radicals and photo-generated holes. Furthermore, the prepared nanocomposite exhibited the superior stability and reusability, successfully performing the AR88 degradation reaction over 7 consecutive cycles.

How to cite this article
Abdulkareem H., Alshujery M., Ahmed M., Shallal W., Hafith A. Preparation of $TiO_2/Cu_{0.4}Fe_{1.6}Ni_{0.65}Zn_{0.35}O_4$ Nanocomposite for Degradation of Acid Red 88 under Visible Light Irradiation. J Nanostruct, 2026; 16(2):2338-2347. DOI: 10.22052/JNS.2026.02.077

INTRODUCTION

With the escalating issue of water pollution, we are facing an environmental catastrophe [1]. Not only human, but other beings are affected by pollution of oceans and seas [2]. Human activities are a leading cause for this crisis, and annually sheer volume of toxic compounds including industrial, agricultural, and municipal wastewater are released into environment [3, 4]. As a consequence, numerous life-threatening diseases have emerged, and the sustainability of our food supply is under threat due to water pollution. Therefore, governments and health agencies around the world are spending billion dollars to mitigate these problems [5, 6].

* Corresponding Author Email: dr.waleedkut@gmail.com

Fortunately, we have a potential complement to clean water resources, employing photocatalysis method [7, 8]. According to its methodology, photocatalysis is defined by light-activated catalyst, which produces highly reactive oxidative species [9, 10]. These species, including hydroxyl ($OH^{\bullet}$) and superoxide ($O_2^{\bullet -}$) radicals, are sufficiently strong to degrade pollutants. Titanium dioxide (TiO_2) and zinc oxide (ZnO) are two major photocatalysts, which have been widely used. However, low quantum efficiency of TiO_2 and ZnO caused by limited lifetime of photo-generated electrons and holes is a main obstacle to harness photocatalytic method for degradation of pollutants [11-13].

In order to effectively utilize photocatalysis for water purification, it is important to have a superior photocatalyst. Recently, many efforts have been devoted to make an efficient photocatalyst, operating under visible light irradiation [14, 15]. Mixed metal oxides have occupied a prominent position in this regard [16]. Owing to the facilitated electron transitions across the energy levels on the different components, the quantum yield of photocatalyst increases as high as possible [17]. These electronic transitions significantly decrease recombination of the charge carriers—photo-generated electrons and holes—thereby increase their lifetime for participating in the pollutant degradation process [18, 19].

For example, Zhang et al. reported the photocatalytic activity of $CuBi_2O_4$/$CdMoO_4$ for degradation of methylene blue [20]. Peng et al. synthesized MgAlO/$MgCr_2O_4$ as a mixed metal oxide photocatalyst to oxidize cyclohexane [21]. A ternary mixed metal oxide nanocomposite comprising of Ag_2O/NiO/ZnO was synthesized for removal of organic pollutant by Bhatia et al. [22].

In this study, TiO_2/$Cu_{0.4}Fe_{1.6}Ni_{0.65}Zn_{0.35}O_4$ nanocomposite (TiO_2/CFNZO) was prepared via two-step synthetic route. First, a co-precipitation reaction was used to prepare $Cu_{0.4}Fe_{1.6}Ni_{0.65}Zn_{0.35}O_4$ nanoparticles (CFNZO) in the presence of polyethylene glycol (PEG) as capping agent. Then, the prepared CFNZO nanoparticles were added to an as-prepared TiO_2 sol solution and the TiO_2/CFNZO nanocomposite was prepared by sol-gel reaction. The nanocomposite is expected to serve as the photocatalyst for removal of aqueous solution of acid red 88 (AR88) under visible light source. Therefore, the photocatalytic degradation of AR88 was investigated using by added different amounts of TiO_2/CFNZO nanocomposite under the visible light irradiation. Moreover, the degradation efficiency was studied under other experimental conditions, including varied pH of AR88, different H_2O_2 concentration, and different radical scavenger agents.

MATERIALS AND METHODS

Preparation of $Cu_{0.4}Fe_{1.6}Ni_{0.65}Zn_{0.35}O_4$ nanoparticles (CFNZO)

The CFNZO nanoparticles was synthesized using the co-precipitation method. To this end, 1.0 g of polyethylene glycol (PEG) was added to the 100 mL of deionized water, and the metal precursors were added, including $Zn(NO_3)_2.4H_2O$ (0.35 mmol), $Cu(NO_3)_2.3H_2O$ (0.4 mmol), $Fe(NO_3)_3.9H_2O$ (1.6 mmol), and $Ni(NO_3)_2.6H_2O$ (0.65 mmol). The obtained solution was stirred for 30 min. Then, the pH of solution was adjusted to around 9 using addition of NaOH (0.1 M) and stirring was performed for another 30 min. The precipitated product was then collected by centrifugation at 6000 rpm for 10 min and washed several times using 20% (V/V) ethanol solution. Finally, the obtained solid was dried overnight in an oven at 100 °C and then calcined at 600 °C for 7 h.

Preparation of TiO_2/$Cu_{0.4}Fe_{1.6}Ni_{0.65}Zn_{0.35}O_4$ nanocomposite (TiO_2/CFNZO)

The TiO_2/CFNZO nanocomposite was prepared via sol-gel route, as follows: First, 1 mmol of tetrabutyl orthotitanate (TBOT) was added into 50 mL of absolute ethanol, and then appropriate amount of the as-prepared CFNZO nanoparticles (2, 4, and 6 wt%) was added and the mixture was stirred for 2 h. The mixture was dried at 90 °C for 24 h and then calcined at 600 °C for 7 h. The nanocomposites comprising 2wt%, 4wt%, and 6wt% of the CFNZO nanoparticles were signified as TiO_2/2-CFNZO, TiO_2/4-CFNZO, and TiO_2/6-CFNZO, respectively.

Characterization

Surface morphology and elemental composition of the prepared nanocomposite were analyzed via scanning electron microscope (SEM, TESCAN Mira3). Phase structure of nanocomposite was investigated using X-ray diffraction analysis (XRD, Philips Pro MPD). Light absorption properties of the prepared nanocomposite was studied using diffuse reflectance spectroscopy (DRS) by JASCO UV/Vis spectrophotometer. Also, photoluminescence (PL) spectroscopy by PL CARY ECLIPSE to further investigate the optical properties.

Photocatalytic studies

The photocatalytic activity of the prepared TiO_2/CFNZO nanocomposite was tested using degradation of acid red 88 (AR88) solution (50 ppm) under LED light (50 W, $\lambda > 500$ nm) irradiation. The photocatalytic tests were initially performed in the darkness under stirring for 30 min. It is important to achieve adsorption/desorption equilibrium between nanocomposite particles and AR88 molecules. Then, illumination was carried out from a distance of 25 cm for 120 min, and every 30 min the degradation of AR88 was investigated using VU/Vis spectroscopy at maximum wavelength (506 nm) of AR88 solution.

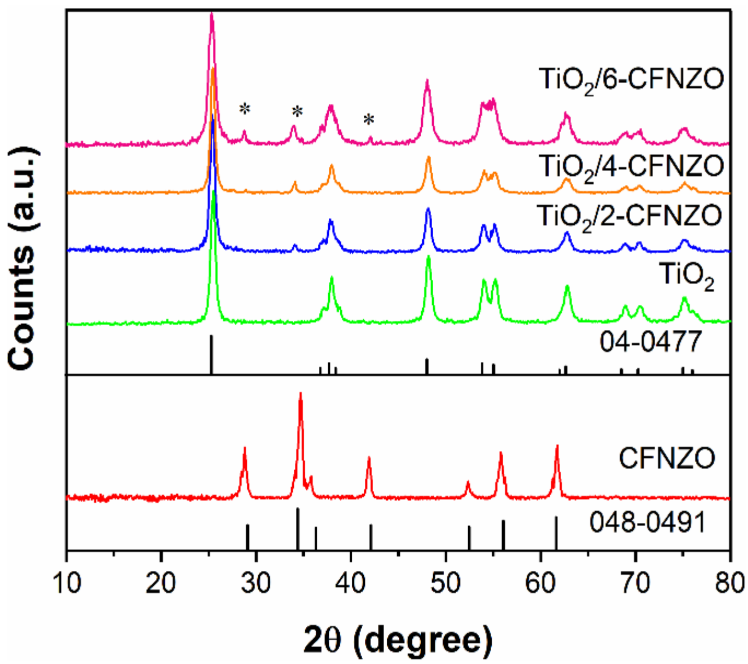

Fig. 1. XRD patterns for pure CFNZO, pure TiO_2, and different prepared TiO_2/CFNZO nanocomposites.

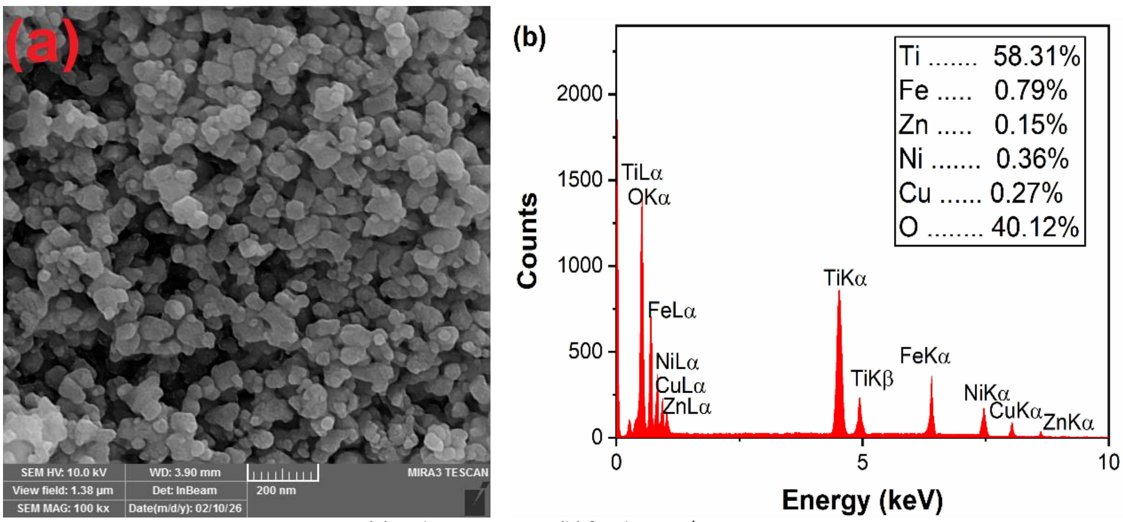

Fig. 2. SEM image (a) and EDX spectrum (b) for the TiO_2/2-CFNZO nanocomposite.

To study the photocatalytic efficiency of the TiO_2/CFNZO nanocomposite under different experimental conditions, the tests were conducted in the presence of different concentrations of H_2O_2 and various radical scavenger agents. Also, the effect of pH of the AR88 was studied on the photocatalytic activity of the TiO_2/CFNZO nanocomposite.

RESULTS AND DISCUSSION

XRD analysis

Fig. 1 represents the XRD patterns for the pure CFNZO and TiO_2 nanoparticles along with TiO_2/CFNZO nanocomposite incorporated with different concentration of CFNZO nanoparticles. The XRD pattern for the CFNZO nanoparticles revealed the cubic structure for the prepared nanoparticles (JCPDS: 048-0491). The observed diffraction peaks at 2θ = 29.45°, 34.73°, 36.61°, 42.45°, 52.84°, 56.44°, and 62.09° are clearly matched with the aforementioned reference code for the $Cu_{0.4}Fe_{1.6}Ni_{0.65}Zn_{0.35}O_4$ compound. As for TiO_2 nanoparticles, the anatase structure was confirmed for the prepared TiO_2 nanoparticles (JCPDS: 04-0477), showing the peaks at 2θ = 25.34°, 36.86°, 37.78°, 38.49°, 48.11°, 53.91°, 55.12°, 62.11°, 62.69°, 68.57°, 70.31°, 75.08°, and 76.11°. The prepared nanocomposite mainly shows the reflections belonged to the TiO_2 phase. The diffraction peaks at around 29.4°, 34.7°, and 42.4° (marked with *) are attributed to the incorporated CFNZO nanoparticles. As the concentration of CFNZO incorporated into the TiO_2 matric increased, the intensity of the associated peaks also increased.

SEM image

The SEM image of the TiO_2/2-CFNZO

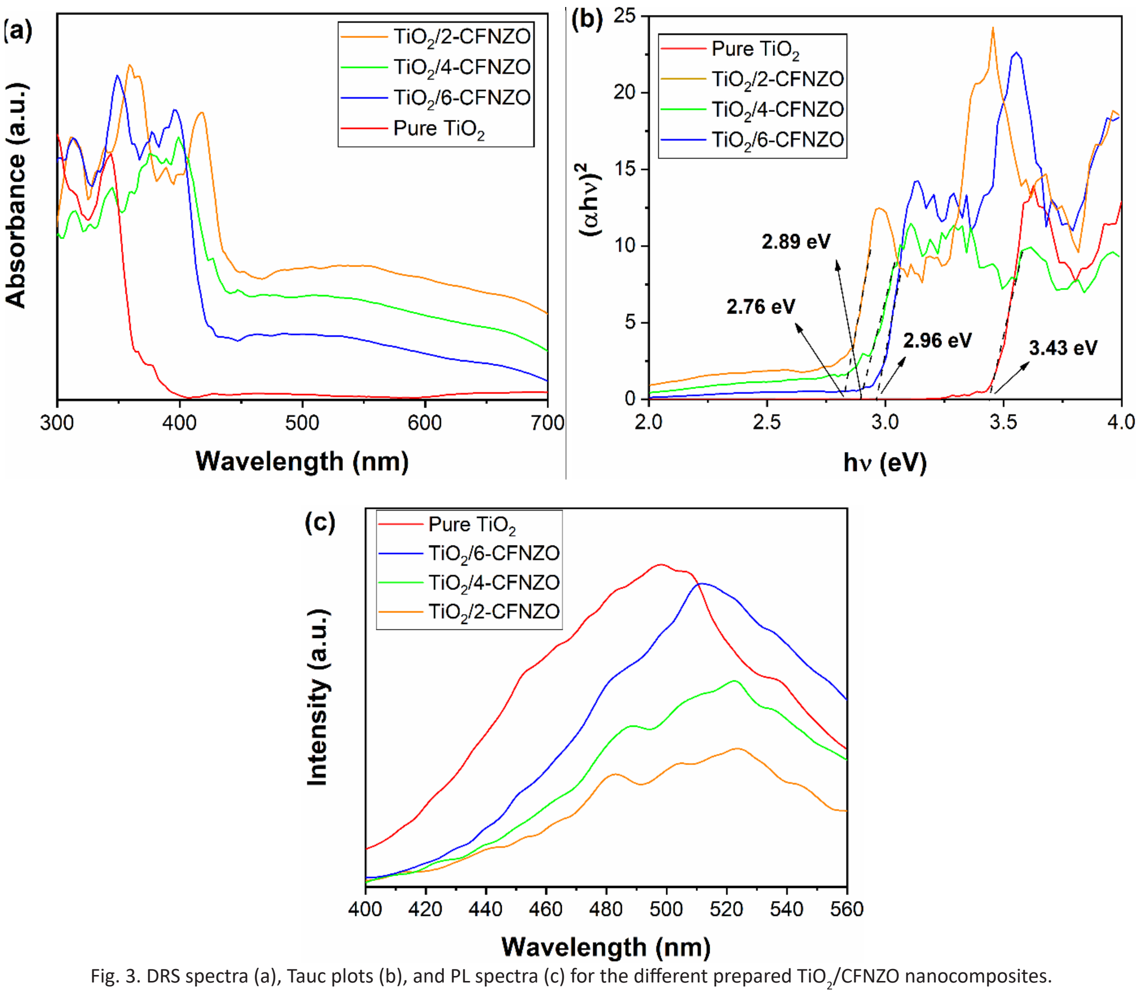

Fig. 3. DRS spectra (a), Tauc plots (b), and PL spectra (c) for the different prepared TiO_2/CFNZO nanocomposites.

nanocomposite was shown in Fig. 2a, exhibiting the semi-spherical nanoparticles with the size in the range 50-100 nm. In addition, the composition and microanalysis of the nanocomposite were carried out using energy dispersive X-ray (EDX) spectroscopy, shown in Fig. 2b. As depicted, the nanocomposite is consisted of Ti (58.31%), Fe (0.79%), Zn (0.15%), Ni (0.36%), Cu (0.27%), and O (40.12%).

DRS and PL analyses

Optical properties of the TiO_2/CFNZO nanocomposite were studied using DRS and PL spectroscopy. Fig. 3a exhibits the absorption of the nanocomposite, revealing the TiO_2/2-CFNZO possesses the higher absorption in the visible light region (400-700 nm). However, no enhancement in the absorption was observed by incorporation of CFNZO by 4 wt% and 6 wt%. This result confirmed that the 2% of the CFNZO nanoparticles effectively contribute to enhance the separation of charge carriers, thereby TiO_2/2-CFNZO nanocomposite shows the higher visible light photoactivity. Additionally, the optical band gaps were determined for the nanocomposites as 2.76, 2.89, and 2.96 eV for the TiO_2/2-CFNZO, TiO_2/4-CFNZO, and TiO_2/6-CFNZO, respectively. In comparison to the prepared nanocomposite, pure TiO_2 has the band gap of 3.43 eV.

For further confirmation of the potential of CFNZO nanoparticles for the enhancement of the photocatalytic activity of TiO_2, PL analysis was performed to study the separation efficiency of the electron/hole pairs. The results revealed that the incorporation of 2% of CFNZO nanoparticles led to the significant decrease of the PL intensity, implying that the suppressed radiative recombination of the electron hole pairs. However, PL intensity was not positively affected by more amounts of the CFNZO nanoparticles.

Photocatalytic tests

The Photocatalytic performance of the different prepared TiO_2/CFNZO nanocomposites (0.04 g) was studied by the visible-light removal of AR88 solution. Fig. 4 shows the performance of the TiO_2/CFNZO nanocomposite for the AR88 degradation under 120 min the visible light irradiation. As seen, the TiO_2/2-CFNZO nanocomposite represents the optimal performance (90.7%) of the photocatalytic activity, which is attributed to the enhanced visible-light absorption ability. By comparison, the

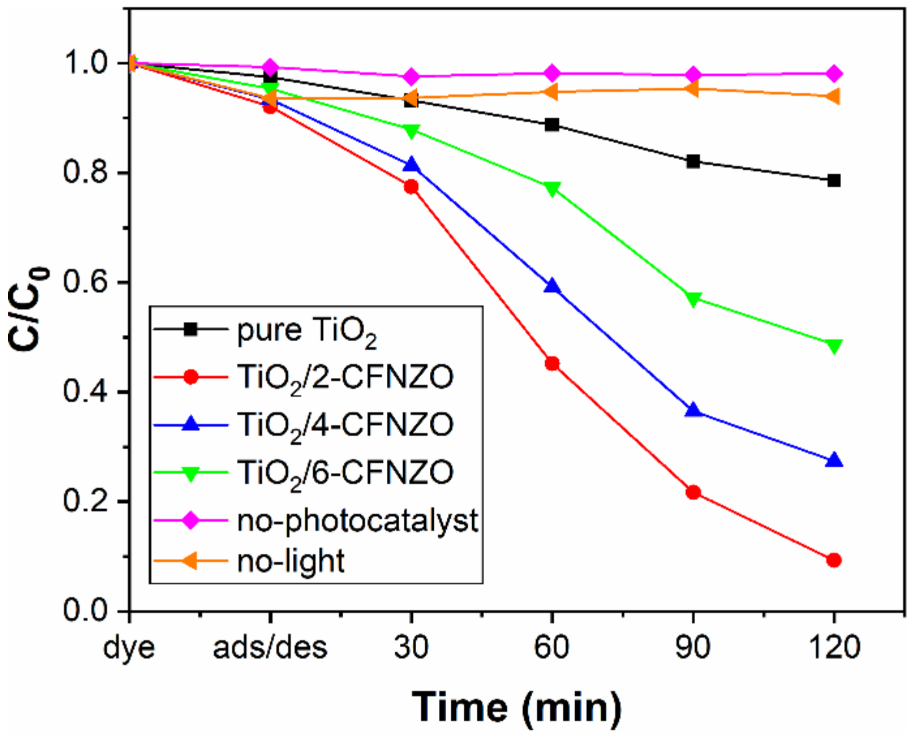

Fig. 4. Photocatalytic degradation of AR88 using different TiO_2/CFNZO nanocomposites.

TiO_2/4-CFNZO and TiO_2/6-CFNZO nanocomposites showed 72.6% and 51.3% of the AR88 degradation during the same irradiation time, respectively. The pure TiO_2 was able to degrade the AR88 solution by only 21.4%. Additionally, the degradation yield of the AR88 was insignificant under no catalyst condition, revealing that the AR88 is stable under the visible light irradiation and represents negligible degradation in the absence of the TiO_2/CFNZO nanocomposite. Similarly, when no visible light source was used, the degradation of AR88 was too low, which is confirmed that the reported degradation efficiency of AR88 solution can be truly attributed to the photocatalytic reaction over the TiO_2/CFNZO nanocomposite.

Photocatalyst amount

In order to study the optimal amount of the TiO_2/2-CFNZO nanocomposite to attain the highest photocatalytic yield, different amounts of the

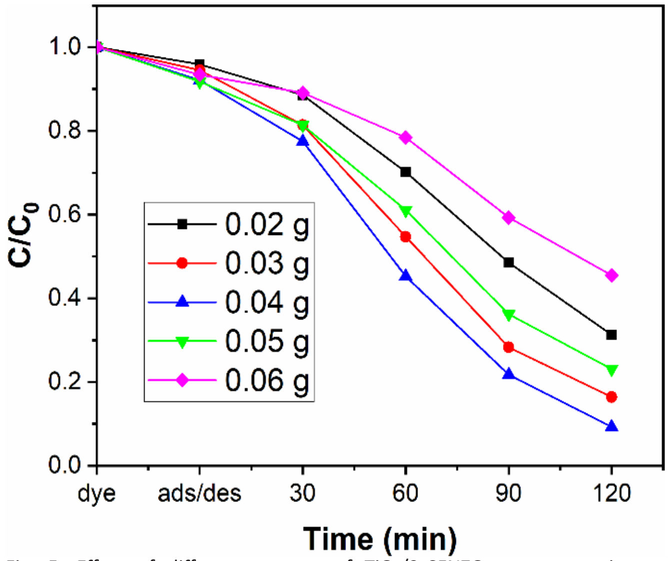

Fig. 5. Effect of different amount of TiO_2/2-CFNZO nanocomposite on degradation level of the AR88 solution.

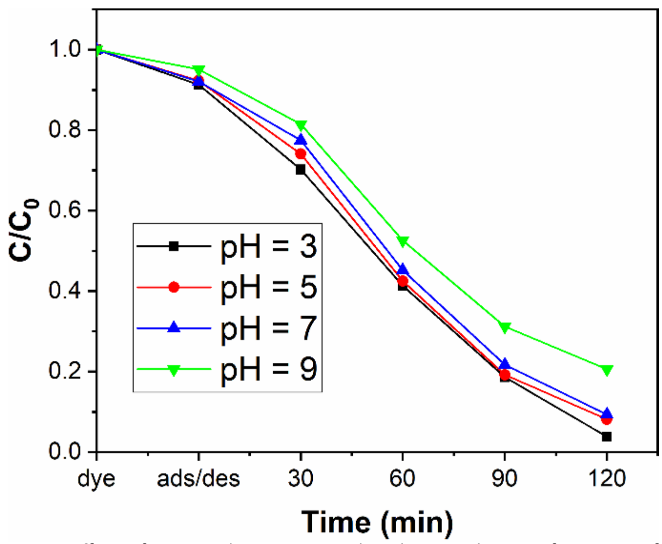

Fig. 6. Effect of AR88 solution pH on the photocatalytic performance of TiO_2/2-CFNZO nanocomposite.

nanocomposite (0.02, 0.03, 0.04, 0.05, and 0.06 g) were loaded and the degradation level of the AR88 was carefully monitored, as shown in Fig. 5. The photocatalytic degradation of AR88 solution reached to the highest level using 0.04 g of theTiO_2/2-CFNZO nanocomposite. As can be seen, the exceeded amount (0.05 and 0.06 g) caused to prominent decrement in the photocatalytic yield. More amount of the loaded photocatalyst, the more active site is. However, when overuse of the photocatalyst leads to a relatively turbid solution, impeding the light beams to penetrate into the solution effectively, and thereby activate the photocatalyst [23-25].

pH of AR88

Fig. 6 shows the effect of pH of the AR88 on the photocatalytic performance of the TiO_2/2-CFNZO nanocomposite. As can be seen, the nanocomposite shows the better result at lower pH values, so that the degradation yield reached to 96.2% at pH of 3. However, the photocatalytic efficiency of the TiO_2/2-CFNZO nanocomposite gradually decreased by increasing the pH values to 9. At pH of 9, the photocatalytic activity of the nanocomposite approached 79.4%. These observations can be justified by concluding that anionic AR88 molecules increasingly adsorb on the positively charged surface of photocatalyst [26-29]. Consequently, AR88 is more oxidized under acidic conditions.

H_2O_2 concentration

The photocatalytic reaction is largely affected by the oxidant agents, due to contribution of oxidants to photocatalytically formation of radicals—$^{\bullet}OH$ or $^{\bullet}O_2^{-}$ [30]. In this work, H_2O_2 was used to elevate the degradation yield of the AR88 solution over the TiO_2/2-CFNZO nanocomposite. Fig. 7 exhibits the impact of the addition of different amounts of H_2O_2 (0.02 M) on the photocatalytic activity of the TiO_2/2-CFNZO nanocomposite. The H_2O_2 had beneficial effect on the photocatalytic activity of the TiO_2/2-CFNZO nanocomposite. More than 98.3% of the AR88 was removed with the addition of 2 mL of H_2O_2 (0.02 M). More amounts of the H_2O_2 (4 mL) led to the dramatic decrease in the photocatalytic activity, which is attributed to the suppression of the formation of radicals during the photocatalytic reactions [31].

Scavenger agents

The photocatalytic experiments were also carried out in the presence of different radical

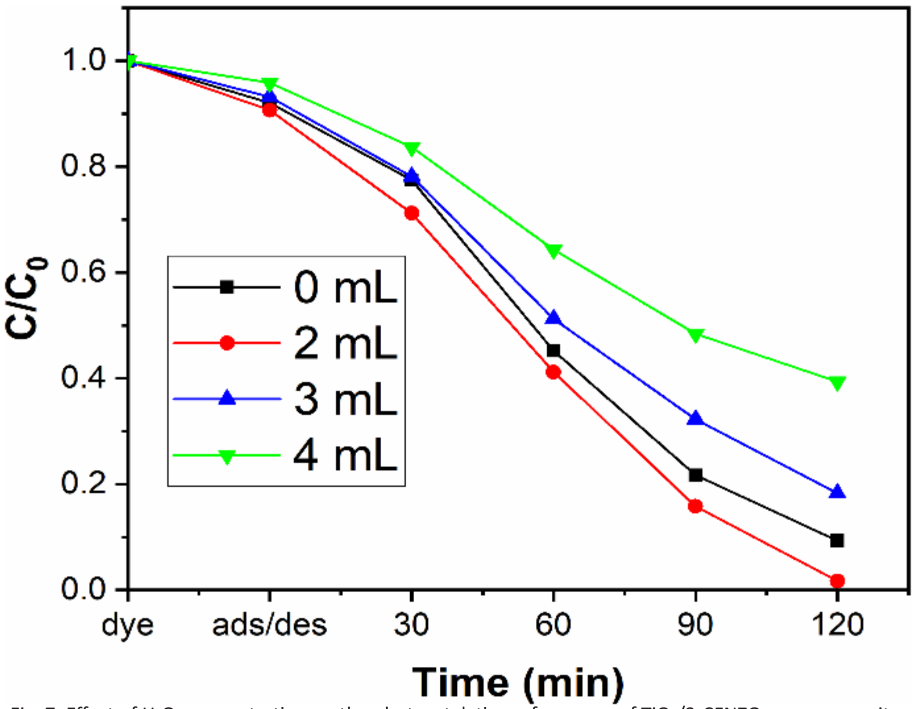

Fig. 7. Effect of H_2O_2 concentration on the photocatalytic performance of TiO_2/2-CFNZO nanocomposite.

scavenger agents, including disodium salt of ethylenediaminetetraacetic acid (EDTA), isopropanol, and ascorbic acid for hindering the photo-generated holes (h^+), hydroxyl radicals ($^{\bullet}OH$), and superoxide radicals ($^{\bullet}O_2^{-}$.), respectively [32-34]. Fig. 8 shows the effects of the addition of (2 mM) different radical scavenger agents on the photocatalytic degradation of AR88 solution. The results showed the photocatalytic activity of the TiO_2/2-CFNZO nanocomposite decreased as EDTA and isopropanol were added, confirming that the photocatalytic degradation of AR88 over the TiO_2/2-CFNZO nanocomposite dominantly performed by $^{\bullet}OH$ radicals and photo-generated h^+.

Reusability tests

The stability of the photocatalyst for multiple uses in an important feature of a practical photocatalyst [35]. In order to study the reusability and structural stability of the prepared TiO_2/2-CFNZO nanocomposite, the photocatalytic degradation reactions were conducted under 7 successive cycles. All the reaction were carried out using the constant amount of the nanocomposite (0.04 g), which was recovered after each reaction cycle by centrifugation at 7000 rpm for 5 min, washed using ethanol solution (20% V/V) and then dried at 90 °C for 4 h. Fig. 9 shows the degradation efficiency of AR88 under 7 successive reactions. As shown, the TiO_2/2-CFNZO nanocomposite

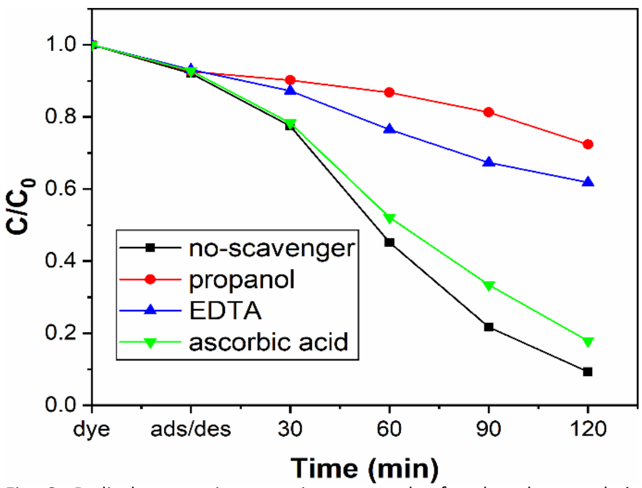

Fig. 8. Radical scavenging experiments results for the photocatalytic degradation of AR88 using TiO_2/2-CFNZO nanocomposite.

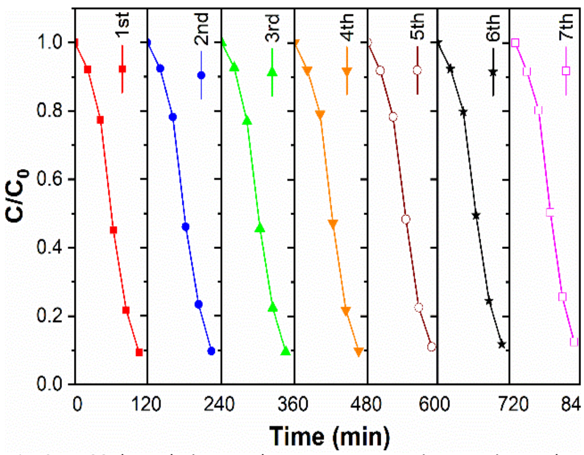

Fig. 9. AR88 degradation results over 7 consecutive reaction cycles using TiO_2/2-CFNZO nanocomposite.

possesses the superior reusability without significant decrease in the degradation efficiency over 7 reaction cycles. After 7th reaction, the decrease in the photocatalytic activity was only 3.28%.

CONCLUSION

In summary, we have prepared TiO_2/$Cu_{0.4}Fe_{1.6}Ni_{0.65}Zn_{0.35}O_4$ nanocomposite using two steps reaction, including co-precipitation and sol-gel methods. The characterization of the nanocomposite was performed to investigate the ability of the nanocomposite to function as the visible-light photocatalyst. The band gap values of the TiO_2/$Cu_{0.4}Fe_{1.6}Ni_{0.65}Zn_{0.35}O_4$ nanocomposites including different concentrations of the CFNZO nanoparticles (2%, 4%, and 6%) were determined to be 2.76, 2.89, and 2.96 eV, respectively. Accordingly, the TiO_2/2-CFNZO nanocomposite was used to study the visible-light removal of AR88 within 120 min photocatalytic reaction. The degradation yield was obtained about 90.7% using 0.04 g of the prepared nanocomposite. Additionally, after careful examination, it was found that the prepared nanocomposite showed the better photoactivity in acidic conditions and in the presence of H_2O_2 (2 mL, 0.02 M). The radical scavenging experiments also exhibited that the degradation of AR88 was accomplished using hydroxyl radicals and photo-generated holes. Furthermore, the prepared nanocomposite showed the superior photocatalytic activity over 7 consecutive reaction cycles, without significant loss of photocatalytic performance.

CONFLICT OF INTEREST

The authors declare that there is no conflict of interests regarding the publication of this manuscript.

REFERENCES

1. García-Ávila F, Rojas-Yanzaguano M, Roldán-Lata A, Valdiviezo-Gonzales L, Alfaro-Paredes E, Avilés-Añazco A. Adaptive management strategies for the improvement of water quality and sustainability in water recharge areas. Sustainable Futures. 2026;11:101610.
2. Zhou Y, Gu B. The impacts of human activities on Earth Critical Zone. Earth Critical Zone. 2024;1(1):100004.
3. Rajaram P, Shanmugapriya D, Mani D, Alharthi FA, Vignesh S. Sustainable synthesis of dual-functional 1D α-MoO3 nanorods for efficient photocatalytic detoxification of various environmental emerging pollutants and antimicrobial activity. Mater Res Bull. 2026;200:114071.
4. Kuriechen SK, Murugesan S. Carbon-Doped Titanium Dioxide Nanoparticles Mediated Photocatalytic Degradation of Azo Dyes Under Visible Light. Water, Air, and Soil Pollution. 2013;224(9).
5. Song Y, Hou D, Zhang J, O'Connor D, Li G, Gu Q, et al. Environmental and socio-economic sustainability appraisal of contaminated land remediation strategies: A case study at a mega-site in China. Sci Total Environ. 2018;610-611:391-401.
6. Condit W, Hawley E, Rectanus H, Deeb R. Global trends in the environmental remediation industry. J Environ Manage. 2017;204:705-708.
7. Kunarti ES, Agustiningsih D, Pambudi FI, Rusli S, Rusdiarso B. Silver-and-Sulphur-Codoped Fe_3O_4/TiO_2 as a Magnetically Separable Photocatalyst for Methylene Blue Degradation under Visible Light. Molekul. 2024;19(1):143.
8. Sikiru S, Busari YO, Olutoki JO, Kumar N, Giri J, Rotimi BI, et al. Polymer Photocatalysts for Green Energy and Environmental Remediation: Recent Progress, Challenges, and Future Directions. Results in Engineering. 2026;29:108976.
9. Pang AL, Arsad A, Ahmad Zaini MA, Garg R, Saqlain Iqbal M, Pal U, et al. A comprehensive review on photocatalytic removal of heavy metal ions by polyaniline-based nanocomposites. Chem Eng Commun. 2023;211(2):275-299.
10. Oladipo AA. $CuCr_2O_4$@CaFe–LDO photocatalyst for remarkable removal of COD from high-strength olive mill wastewater. Journal of Colloid and Interface Science. 2021;591:193-202.
11. Daghrir R, Drogui P, Robert D. Modified TiO_2 For Environmental Photocatalytic Applications: A Review. Industrial and Engineering Chemistry Research. 2013;52(10):3581-3599.
12. Ahmad I, Shukrullah S, Naz MY, Ahmad M, Ahmed E, Liu Y, et al. Recent advances and challenges in 2D/2D heterojunction photocatalysts for solar fuels applications. Advances in Colloid and Interface Science. 2022;304:102661.
13. Croxall MP, Lawrence RT, Ghosh Biswas R, Soong R, Simpson AJ, Goh MC. Improved Photocatalytic Performance of TiO_2–Nitrogen-Doped Graphene Quantum Dot Composites Mediated by Heterogeneous Interactions. The Journal of Physical Chemistry Letters. 2024;15(13):3653-3657.
14. Samarasinghe LV, Muthukumaran S, Baskaran K. Recent advances in visible light-activated photocatalysts for degradation of dyes: A comprehensive review. Chemosphere. 2024;349:140818.
15. Olatunde OC, Yusuf TL, Mabuba N, Onwudiwe DC, Makgato S. Interfacial electron redistribution in 2D/3D MoS_2/$CuBi_2O_4$ p-n heterojunction for visible light assisted reduction of Cr(VI) and oxidation of antibiotics. Journal of Water Process Engineering. 2024;59:105074.
16. Azalok KA, Oladipo AA, Gazi M. Hybrid MnFe-LDO–biochar nanopowders for degradation of metronidazole via UV-light-driven photocatalysis: Characterization and mechanism studies. Chemosphere. 2021;268:128844.
17. Basumatary B, Basumatary R, Ramchiary A, Konwar D. Evaluation of Ag@TiO_2/WO_3 heterojunction photocatalyst for enhanced photocatalytic activity towards methylene blue degradation. Chemosphere. 2022;286:131848.
18. Ghamarpoor R, Fallah A, Jamshidi M. A Review of Synthesis Methods, Modifications, and Mechanisms of ZnO/TiO_2-Based Photocatalysts for Photodegradation of Contaminants. ACS Omega. 2024;9(24):25457-25492.
19. Muñoz-Batista MJ, Gómez-Cerezo MN, Kubacka A, Tudela D, Fernández-García M. Role of Interface Contact in CeO_2–TiO_2 Photocatalytic Composite Materials. ACS Catalysis.

2013;4(1):63-72.
20. Zhang X, Wang S, Lin L, Tan X, Zeng Y. Design of a novel CuBi2O4/CdMoO4 heterojunctions with nano-microsphere structure: Synthesis and photocatalytic degradation mechanism. Colloids Surf Physicochem Eng Aspects. 2021;614:126008.
21. Peng D, Zhang Y. Engineering of mixed metal oxides photocatalysts derived from transition-metal-based layered double hydroxide towards selective oxidation of cyclohexane under visible light. Applied Catalysis A: General. 2023;653:119067.
22. Bhatia P, Nath M. Nanocomposites of ternary mixed metal oxides (Ag_2O/NiO/ZnO) used for the efficient removal of organic pollutants. Journal of Water Process Engineering. 2022;49:102961.
23. Ali AT, Guda MA, Oraibi AI, Salih IK, Shather AH, Abd Ali AT, et al. Fe_3O_4 supported [Cu(ii)(met)(pro-H)$_2$] complex as a novel nanomagnetic catalytic system for room temperature C–O coupling reactions. RSC Advances. 2023;13(32):22538-22548.
24. Galedari M, Mehdipour Ghazi M, Rashid Mirmasoomi S. Photocatalytic process for the tetracycline removal under visible light: Presenting a degradation model and optimization using response surface methodology (RSM). Chem Eng Res Des. 2019;145:323-333.
25. Sathish Kumar PS, Sivakumar R, Anandan S, Madhavan J, Maruthamuthu P, Ashokkumar M. Photocatalytic degradation of Acid Red 88 using Au–TiO_2 nanoparticles in aqueous solutions. Water Res. 2008;42(19):4878-4884.
26. Azeez F, Al-Hetlani E, Arafa M, Abdelmonem Y, Nazeer AA, Amin MO, et al. The effect of surface charge on photocatalytic degradation of methylene blue dye using chargeable titania nanoparticles. Sci Rep. 2018;8(1).
27. Trandafilović LV, Jovanović DJ, Zhang X, Ptasińska S, Dramićanin MD. Enhanced photocatalytic degradation of methylene blue and methyl orange by ZnO:Eu nanoparticles. Applied Catalysis B: Environmental. 2017;203:740-752.
28. Waghchaure RH, Adole VA, Jagdale BS. Photocatalytic degradation of methylene blue, rhodamine B, methyl orange and Eriochrome black T dyes by modified ZnO nanocatalysts: A concise review. Inorg Chem Commun. 2022;143:109764.
29. Rahbar M, Mehrzad M, Behpour M, Mohammadi-Aghdam S, Ashrafi M. S, N co-doped carbon quantum dots/TiO_2 nanocomposite as highly efficient visible light photocatalyst. Nanotechnology. 2019;30(50):505702.
30. Gaya UI, Abdullah AH. Heterogeneous photocatalytic degradation of organic contaminants over titanium dioxide: A review of fundamentals, progress and problems. Journal of Photochemistry and Photobiology C: Photochemistry Reviews. 2008;9(1):1-12.
31. Wang Y, Hong C-s. Effect of hydrogen peroxide, periodate and persulfate on photocatalysis of 2-chlorobiphenyl in aqueous TiO_2 suspensions. Water Res. 1999;33(9):2031-2036.
32. Puga F, Navío JA, Hidalgo MC. A critical view about use of scavengers for reactive species in heterogeneous photocatalysis. Applied Catalysis A: General. 2024;685:119879.
33. Rahbar M, Hosseini-Sarvari M. Natural sunlight-driven photocatalytic mineralization of petrochemical wastewater using ceramic-supported Fe, B co-doped TiO_2/CNT@WO_3 in a flat panel photoreactor. Journal of Water Process Engineering. 2025;77:108328.
34. Xiang Q, Yu J, Wong PK. Quantitative characterization of hydroxyl radicals produced by various photocatalysts. Journal of Colloid and Interface Science. 2011;357(1):163-167.
35. Shirazi P, Rahbar M, Behpour M, Ashrafi M. La_2MnTiO_6 double perovskite nanostructures as highly efficient visible light photocatalysts. New J Chem. 2020;44(1):231-238.